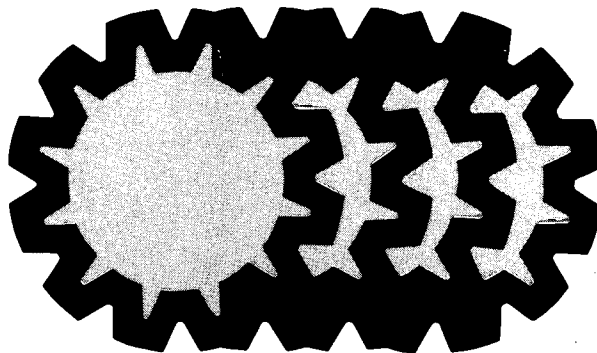


Glaser

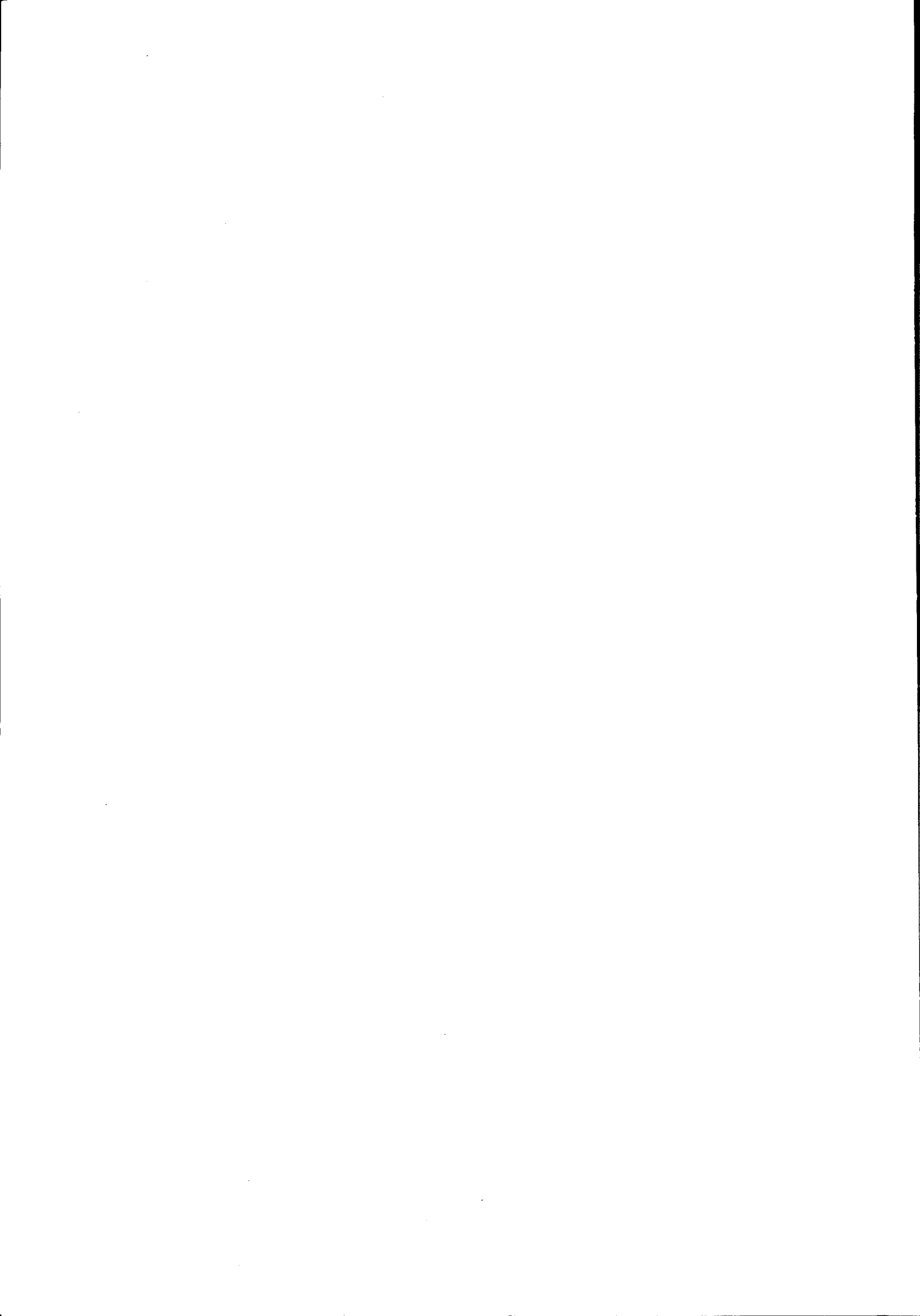
NIOSH

TECHNICAL INFORMATION

Measurement of RF Power-Absorption in Biological Specimens



U.S. DEPARTMENT OF HEALTH, EDUCATION, AND WELFARE / Public Health Service
Center For Disease Control / National Institute For Occupational Safety And Health



MEASUREMENT OF RF POWER-ABSORPTION IN BIOLOGICAL SPECIMENS
(10 to 100 MHz)

Frank M. Greene
Electromagnetics Division
National Bureau of Standards
Boulder, Colorado 80302

Interagency Agreement NIOSH-IA-75-16

U.S. DEPARTMENT OF HEALTH, EDUCATION, AND WELFARE
Public Health Service
Center for Disease Control
National Institute for Occupational Safety and Health
Division of Biomedical and Behavioral Science
Cincinnati, Ohio 45226

February 1977

The contents of this report are reproduced herein as received from the performing agency except for the addition of a disclaimer page, a title page, and table of contents. The opinions, findings, and conclusions expressed are those of the author and not necessarily those of NIOSH. Mention of company or product names is not to be considered as an endorsement by NIOSH.

NIOSH Project Officer: David L. Conover, Ph.D.

DHEW (NIOSH) Publication No. 77-146

MEASUREMENT OF RF POWER-ABSORPTION IN BIOLOGICAL SPECIMENS
(10 to 100 MHz)

Frank M. Greene
Electromagnetics Division
National Bureau of Standards
Boulder, Colorado 80302

ABSTRACT

A method is described for accurately determining the rf power being absorbed by a biological specimen during non-ionizing radiation-exposure testing using the NBS RF Near-Field Synthesizer in the frequency range 10 to 100 MHz. This method is based solely on measuring the forward and reflected power on the transmission line feeding the synthesizer. Commercially available rf wattmeters can be used, and an automatic data-acquisition system employed, if desired, to "read" the meters and rapidly calculate, display, and record the rf power flow.

The method has the advantage that the exact measuring point on the feed line is not critical, as it is with methods employing direct impedance measurements, and that the required measurements can be made without interfering with the exposure tests.

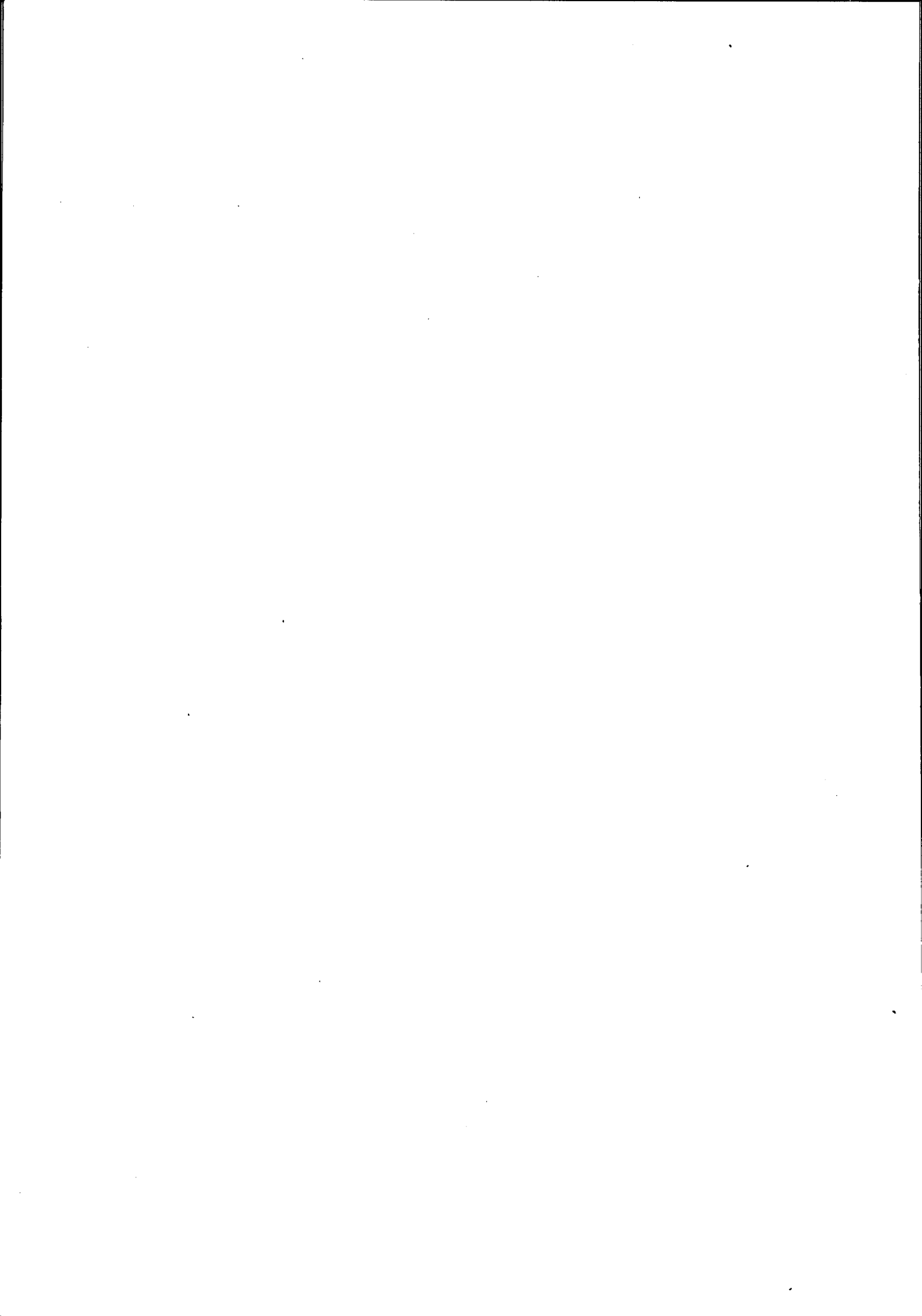
Key words: Electromagnetic field hazards; electromagnetic field synthesizer; electromagnetic radiation-exposure testing (non-ionizing); near-fields; rf biological hazards.

NBS Project 2763281
January 15, 1977



CONTENTS

ABSTRACT-----	iii
INTRODUCTION-----	1
THEORY-----	2
2.1 Introduction-----	2
2.2 Forward and Reflected Power-----	3
2.3 Analysis of the Field Generator-----	4
MEASUREMENT APPLICATIONS-----	9
3.1 Key Equations and Curves-----	9
3.2 Measurement Example-----	9
OPERATING PROCEDURE-----	13
MEASUREMENT SENSITIVITY-----	14
5.1 Basic Sensitivity-----	14
5.2 Increasing the Sensitivity-----	14
MAGNETIC-INDUCTION HEATING IN A LOSSY DIELECTRIC-----	18
6.1 Introduction-----	18
6.2 Theoretical Background-----	18
6.3 RF Heating Density-----	20
6.4 Total RF Heating-----	20
THE CALORIMETER METHOD-----	22
CONCLUSIONS-----	23
REFERENCES-----	24



1. INTRODUCTION

A method will be described for determining the total amount of rf power being absorbed by a biological specimen during non-ionizing radiation-exposure testing using the NBS RF Near-Field Synthesizer in the frequency range 10 to 100 MHz [1]. This method is based solely on measuring the forward and reflected power on the transmission line feeding the field synthesizer. Commercially available rf wattmeters and an automatic data-acquisition system can be employed to further simplify the procedure.*

The near-field synthesizer is installed and operated in a doubly-shielded copper room having a shielding efficiency of 60 dB or more. Any electromagnetic radiation from the synthesizer or test specimen is reduced by a factor of at least 10^6 by the shielding. Radiation losses are therefore considered to be completely negligible. Coupling between the synthesizer and the interior copper walls of the shielded room has been found to be essentially reactive. Very little resistance is coupled back into the synthesizer from the walls of the room.

The rationalized mks International System of Units (SI) is used throughout this report.

*This report is the outgrowth of work originally sponsored by the USAF School of Aerospace Medicine at Brooks AF Base, and the National Institute for Occupational Safety and Health of the Department of HEW.

2. THEORY

2.1 Introduction. The NBS RF Near-Field Synthesizer consists of both an electric-field, and a magnetic-field generator. These two field generators consist of a balanced parallel-plate stripline and a balanced four-gap single-turn loop inductor for generating the "wanted" electric and magnetic fields, respectively [1]. Multiple feeds and balanced symmetry are used to minimize the "unwanted" magnetic and electric field components and to permit superposing the "wanted" fields without significant cross coupling. For the sake of producing hazard-level fields with a minimum of driving power, these field generators are resonated. The two generators can be operated simultaneously to produce a large range of values of E/H, or individually [1].

Each field generator has its own driving transmitter (source) and rf feed system, and the two generators can be considered to be operating essentially independently. The analysis that follows applies to each field generator individually. If both field generators are operating simultaneously, the total power absorbed by the biological specimen may be obtained by adding the power absorbed from each field generator. It has been found at NBS and elsewhere [2] that the magnetic field may represent a greater biological hazard than the electric field in the frequency range under consideration here. Therefore, this analysis will probably be used for the most part with the magnetic-field-generator portion of the near-field synthesizer.

The use of steady-state, sinusoidally time-varying rf driving sources is assumed throughout this report. It is not necessary that these sources be matched to their respective feed lines with this method since only the ratio of the reflected power to the forward power is involved. The sources comprise tuned Class-C rf power amplifiers which must be operated with as much as a 5:1 impedance mismatch in order to obtain the required rf power output with a plate efficiency of 75 to 80 percent [3].

2.2 Forward and Reflected Power. Either field generator is fed rf power by means of a reasonably low-loss 50-ohm transmission line. Either field generator can be tuned and adjusted independently to present a 50-ohm load to its feed line at the operating frequency before the biological specimen is put in place. After the specimen is inserted, the rf power that it absorbs can be determined directly in terms of the reflection that it produces.

The quantities to be discussed now are to be measured on the transmission line feeding either field generator. Since only measurements of the component forward and reflected waves are involved, the exact point at which they are measured is not critical on a low-loss line. This is one of the advantages of this method over methods based on direct impedance measurement.

The complex reflection coefficient, Γ , at the receiving end of a uniform lossless transmission line is given by [4,5]

$$\Gamma = \frac{Z_L - Z_0}{Z_L + Z_0} = \frac{Z_L' - 1}{Z_L' + 1}, \quad (1)$$

where $Z_L' = Z_L/Z_0$. Z_L is the load impedance presented by either field generator to its feed line, and Z_0 is the characteristic impedance of the line. For this analysis Z_L and Z_0 are both considered to be resistive as will be discussed later, making Γ real in the limit.

The forward power, P_f , flowing toward the load is given by

$$P_f = \frac{V_f^2}{Z_0}, \quad (2)$$

where V_f is the rms value of the magnitude of the forward-traveling voltage wave.

The reflected power, P_r , flowing back to the source is given by

$$P_r = \frac{V_r^2}{Z_0}, \quad (3)$$

where V_r is the rms value of the magnitude of the backward-traveling (reflected) voltage wave. Also

$$V_r = \Gamma V_f. \quad (4)$$

Therefore, the reflected power is also given by

$$P_r = \frac{\Gamma^2 V_f^2}{Z_0}. \quad (5)$$

The ratio of the reflected power to the forward power is therefore given by

$$\frac{P_r}{P_f} = \Gamma^2. \quad (6)$$

The load power, P_L , actually absorbed by the load, Z_L , is the arithmetic difference between the forward power, P_f , and the reflected power, P_r , if Z_0 is resistive, i.e.,

$$P_L = P_f - P_r. \quad (7)$$

The ratio of the load power to the forward power is given by

$$\frac{P_L}{P_f} = 1 - \Gamma^2, \quad (8)$$

as obtained from eqs. (6) and (7).

2.3 Analysis of the Field Generator. Each field generator can be represented by an equivalent, tapped, parallel-resonant tank circuit, as shown in figure 1. It should be pointed out, however, that the basic results obtained from this model are also valid near resonance when used with transmission-line types, as well as waveguide types of resonators [6], as will be discussed in connection with eq. (11).

From Ohm's law it can be shown, with the aid of figure 1, that the power absorbed by the biological specimen, P_a , and the load power, P_L , are in the same ratio as the internal rf loss resistances involved. That is,

$$\frac{P_a}{P_L} = \frac{R_2}{R_1 + R_2}, \quad (9)$$

where R_1 represents the loss resistance of the field generator itself prior to inserting the biological specimen, and R_2 is the loss resistance coupled into the generator from the biological specimen after retuning.

It is assumed that the presence of the specimen and the subsequent retuning do not cause a sufficient change in the field distribution within the field generator to change its internal metallic losses. This is believed to be a reasonable assumption. The metallic conductivities involved are so high that the form of the fields is unchanged by the losses that result. The total loss can therefore be computed by adding directly the values of the metallic losses and the dielectric losses [7].

The internal resistance of the field generator is transformed at its input terminals at resonance in accordance with the following relationship, valid provided $Q \geq 10$ [8]

$$Z_L \cong \frac{X_1^2}{R}, \quad (10)$$

where, from figure 1, X_1 is the inductive reactance of the shunt matching inductor, and R is the total series rf resistance of the tank circuit. When eq. (10) is substituted into eq. (9) we obtain, after rearranging,

$$\frac{P_a}{P_L} = 1 - \frac{R_1}{R_1 + R_2} = 1 - \frac{Z_L}{Z_0} = 1 - Z'_L, \quad (11)$$

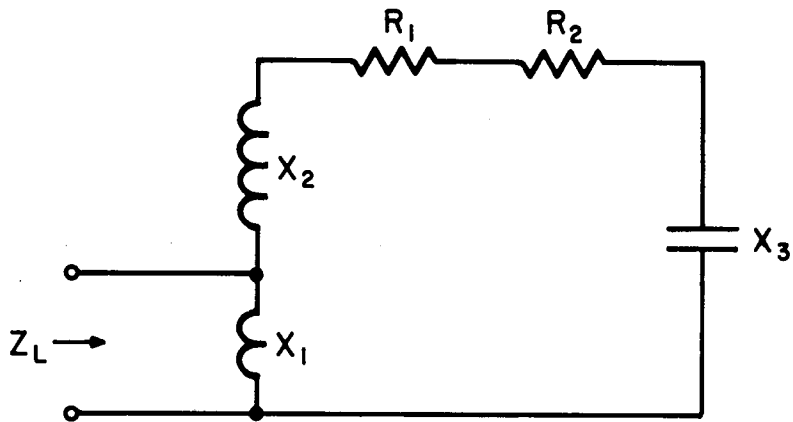


Figure 1. The equivalent lumped-constant circuit diagram of either the electric-field or the magnetic-field generator.

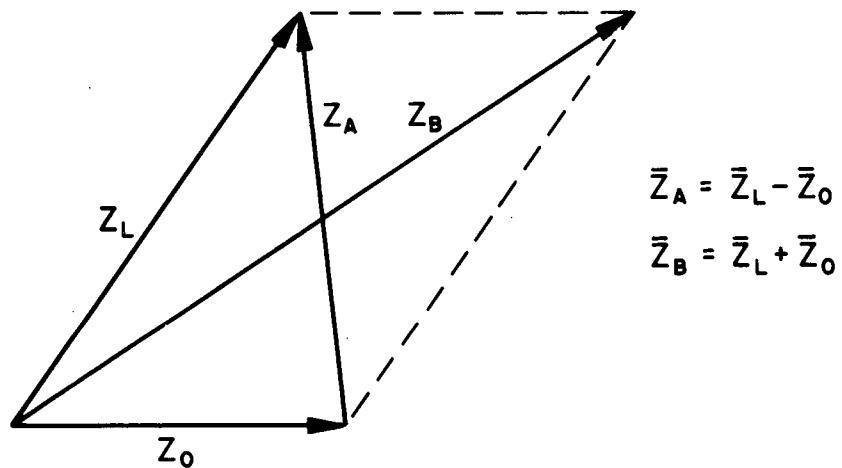


Figure 2. Vector diagram representing the numerator, $\bar{Z}_L - \bar{Z}_0$, and the denominator, $\bar{Z}_L + \bar{Z}_0$, of eq. (1a), where Z_0 is considered to be resistive.

since $Z_L = X_1^2 / (R_1 + R_2)$, and $Z_O = X_1^2 / R_1 = 50$ ohms, from eq. (10), with Z_L' limited to the range $0 \leq Z_L' \leq 1$. Equation (11) shows the basic relationship between the power absorbed by the biological specimen, P_a , and the input impedance of the field generator at resonance, Z_L , and can be used with any type of two-terminal resonator or cavity, as previously mentioned.

In practice, the field generator is first tuned and adjusted for zero reflected power (by adjusting both X_1 and X_3 of figure 1) to give an input impedance of $Z_L = 50$ ohms before the biological specimen is put in place. Afterwards, the field generator is retuned for minimum reflected power (by adjusting X_3 only). This cancels any reactance coupled in from the specimen, making Z_L resistive in both cases as shown in the following paragraph.

The complex receiving-end reflection coefficient is given by eq. (1), rewritten as

$$\bar{\Gamma} = \frac{\bar{Z}_L - \bar{Z}_O}{\bar{Z}_L + \bar{Z}_O} = \frac{\bar{Z}_A}{\bar{Z}_B} \quad (1a)$$

The numerator is the vector difference and the denominator the vector sum of \bar{Z}_L and \bar{Z}_O , as shown in figure 2, where \bar{Z}_O is considered to be resistive. The numerator of eq. (1a) will be a minimum and the denominator a maximum simultaneously when \bar{Z}_L becomes resistive, thus minimizing $\bar{\Gamma}$ as can be readily seen from figure 2.

Solving eq. (1) for Z_L' gives

$$Z_L' = \frac{1 + \Gamma}{1 - \Gamma} \quad (12)$$

Substituting eq. (12) into (11) gives

$$\frac{P_a}{P_L} = \frac{2|\Gamma|}{1 + |\Gamma|} \quad (13)$$

with Γ limited to the range $-1 \leq \Gamma \leq 0$. Using eq. (6), eq. (13) can also be written

$$\frac{P_a}{P_L} = \frac{2\sqrt{P_r/P_f}}{1 + \sqrt{P_r/P_f}}. \quad (14)$$

To obtain the ratio of the power absorbed by the specimen, P_a , to the forward power, P_f , eq. (13) must be multiplied by eq. (8), giving

$$\frac{P_a}{P_f} = 2|\Gamma| [1 - |\Gamma|]. \quad (15)$$

Using eq. (6) again, eq. (15) can also be written

$$\frac{P_a}{P_f} = 2\sqrt{P_r/P_f} \left[1 - \sqrt{P_r/P_f} \right]. \quad (16)$$

Finally, eq. (8) can be included in the form

$$\frac{P_L}{P_f} = 1 - \frac{P_r}{P_f}. \quad (17)$$

3. MEASUREMENT APPLICATIONS

3.1 Key Equations and Curves. Equations (14), (16), and (17) are the key equations to be used in this technique. As can be seen, the power absorbed by the biological specimen, P_a , can be obtained relative to either the load power, P_L , or the forward power, P_f , knowing only the ratio of the reflected power to the forward power, P_r/P_f , as summarized in table I.

Equations (14) and (17) are shown plotted in figure 3 as curves (a) and (b), respectively. Equations (16) and (17) are shown plotted in figure 4 as curves (a) and (b), respectively. It is interesting to note from curve (a) of figure 4 that the power absorbed by the specimen, P_a , can never exceed half of the forward power, P_f . This maximum occurs when the reflected power is 25 percent of the forward power.

3.2 Measurement Example. An example will be given to illustrate the use of the equations and curves. It is assumed that the field generator is first tuned and adjusted for zero reflected power to give an input impedance of 50 ohms before the biological specimen is put in place. Afterwards, the generator is retuned for minimum reflected power to cancel any reactance coupled in from the specimen, as previously discussed.

Example

Assume that the forward power, $P_f = 100$ watts, and the reflected power, $P_r = 11.1$ watts. Then $P_r/P_f = 0.111$. The load power, P_L , can be obtained from eq. (17) or curve (b) of figure 3, if desired, as $P_L = 100 - 11.1 = 88.9$ watts. From eq. (14), or curve (a) of figure 3 (corresponding to $P_r/P_f = 0.111$) the ratio $P_a/P_L = 0.500$. That is, half of the load power, or 44.4 watts, is absorbed by the biological specimen, and the other half goes into heating the field generator. This same value of absorbed power, P_a , can also be obtained directly from eq. (16), or curve (a) of figure 4, giving $P_a/P_f = 0.444$, or $P_a = 44.4$ watts as before.

Table I

RF Power Absorbed by a Biological Specimen

<u>Reflected Power</u>	<u>Load Power</u>	<u>Power Absorbed by Specimen</u>	<u>Power Absorbed by Specimen</u>
Eq. (6)	Eq. (8)	Eq. (14)	Eq. (16)
$\frac{P_r}{P_f} \times 100$	$\frac{P_L}{P_f} \times 100$	$\frac{P_a}{P_L} \times 100$	$\frac{P_a}{P_f} \times 100$
(%)	(%)	(%)	(%)
0.00	100.00	0.00	0.00
0.10	99.90	6.13	6.12
0.20	99.80	8.56	8.54
0.50	99.50	13.21	13.14
1.00	99.00	18.18	18.00
2.00	98.00	24.78	24.28
4.00	96.00	33.33	32.00
6.00	94.00	39.35	36.99
8.00	92.00	44.10	40.57
10.00	90.00	48.05	43.25
11.11	88.89	50.00	44.44
15.00	85.00	55.83	47.46
20.00	80.00	61.80	49.44
25.00	75.00	66.67	50.00
30.00	70.00	70.78	49.54
40.00	60.00	77.49	46.49
50.00	50.00	82.84	41.42
60.00	40.00	87.30	34.92
70.00	30.00	91.11	27.33
80.00	20.00	94.43	18.89
90.00	10.00	97.37	9.74
100.00	0.00	100.00 (a)	0.00

(a) Theoretical limiting value.

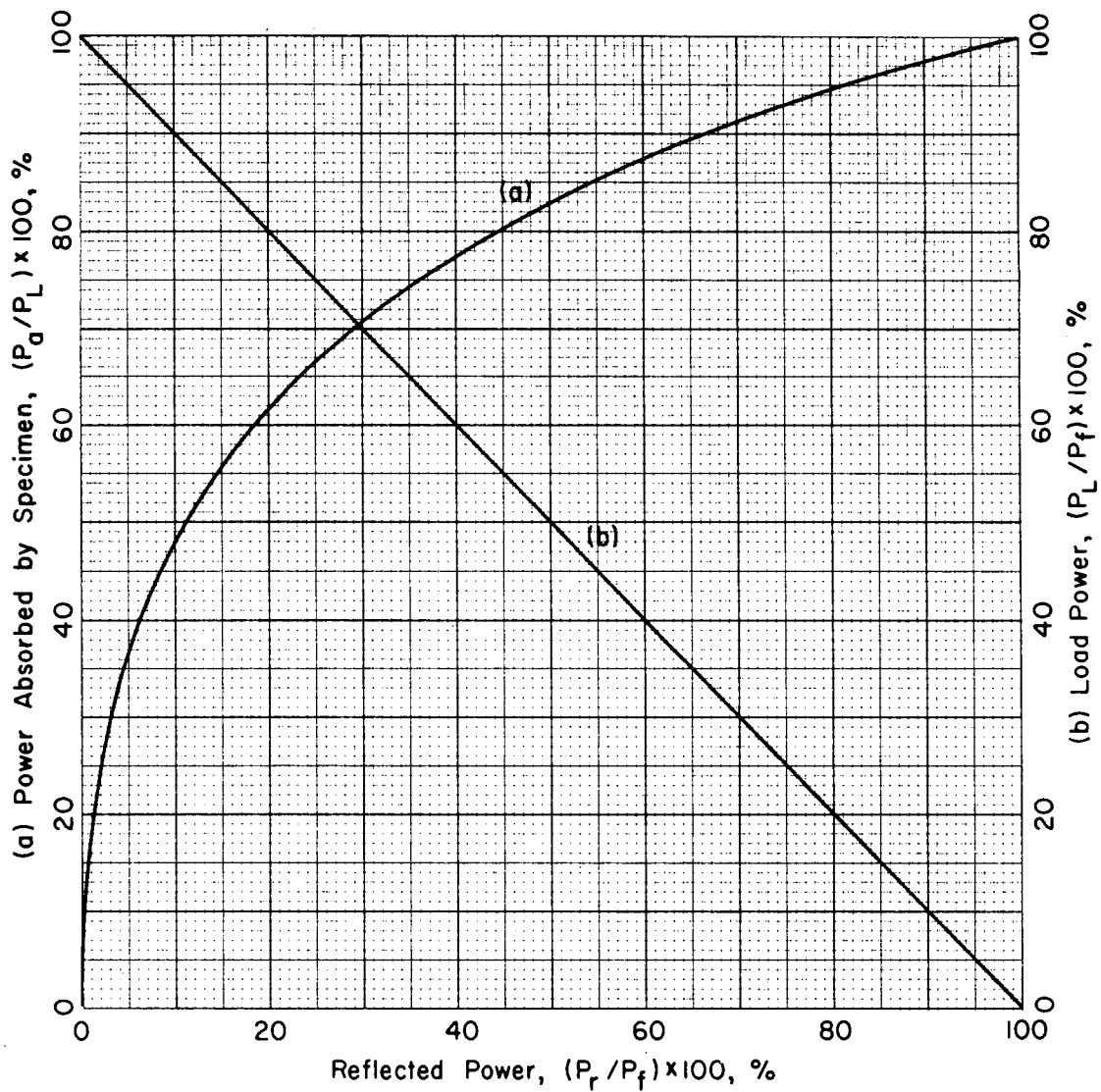


Figure 3. (a) RF power absorbed by the biological specimen, $(P_a/P_L) \times 100, \%$; and (b) load power, $(P_L/P_f) \times 100, \%$; both vs. the reflected power, $(P_r/P_f) \times 100, \%$; where P_f is the forward power in watts.

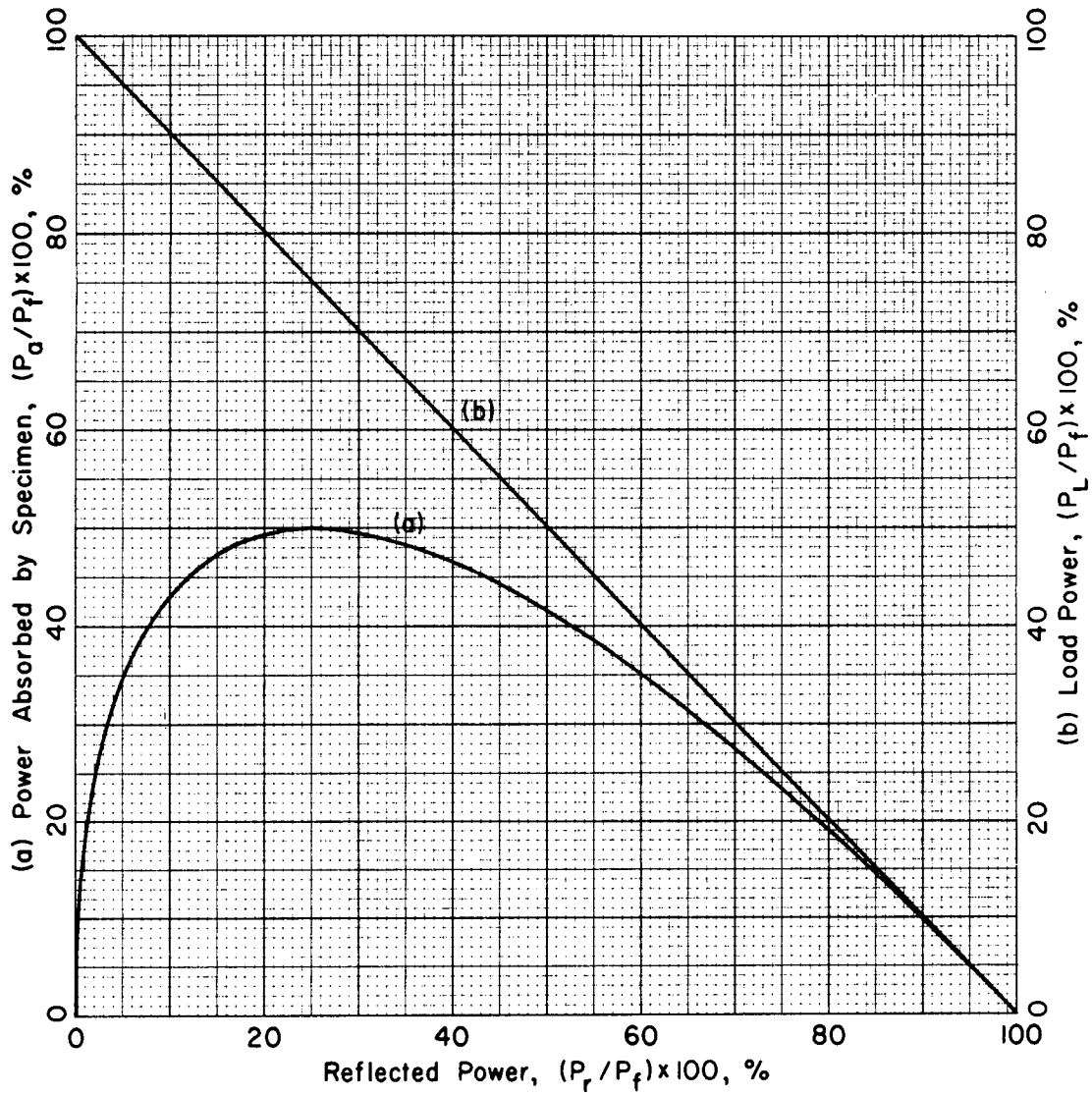


Figure 4. (a) RF power absorbed by the biological specimen, $(P_a/P_f) \times 100, \%$; and (b) load power, $(P_L/P_f) \times 100, \%$; both vs. the reflected power, $(P_r/P_f) \times 100, \%$; where P_f is the forward power in watts.

4. OPERATING PROCEDURE

- (a) The rf directional couplers of the wattmeters being used should be inserted in the feed-line to each field generator, usually within one or two meters of the generator input terminals. The exact location is, however, not critical with this method, as discussed in section 2.2.
- (b) The input channels of the automatic data-acquisition system can be connected directly to the respective dc terminals of the microammeters used to indicate forward and reflected power. Store the calibration data of these wattmeters in the associated computer as part of the data acquisition program (i.e., rf watts input to the coupler vs. dc millivolts output).
- (c) The field generator should be adjusted at the desired operating frequency (in the absence of the biological specimen) in accordance with the usual procedure [1].
- (d) Adjust the generator matching networks for zero reflected power, so that the generator presents a load impedance $Z_L = 50$ ohms to its feed line.
- (e) The rf power input to the field generator should then be reduced and the biological specimen placed at its center.
- (f) The rf power should then be gradually increased and the tuning capacitors of the generator matching units carefully readjusted for minimum reflected power. This cancels the reactance coupled into the field generator from the specimen as discussed in section 2.3
- (g) Read the forward power, P_f , and the reflected power, P_r . Calculate the ratio, P_r/P_f , and the load power, $P_L = P_f - P_r$. The remainder of the calculations should be made as outlined in section 3.2.

5. MEASUREMENT SENSITIVITY

5.1 Basic Sensitivity. The basic measurement sensitivity [9] or resolution, δ , of the method being described is given by the ratio of the reflected power, P_r/P_f , to the power absorbed by the biological specimen, P_a/P_f , at the final operating point on the characteristic curve (eq. (16)), i.e.,

$$\text{Measurement sensitivity} = \delta = \frac{P_r/P_f}{P_a/P_f} . \quad (18)$$

From eq. (16) or curve (a) of figure 4, it can be seen that the measurement sensitivity is zero when $P_a/P_f = 0$, and increases with increasing values of P_a/P_f to a sensitivity of 0.500 when $P_a/P_f = 0.500$, probably the upper limit of the useful measurement range. While the sensitivity is deemed to be adequate over most of the measuring range, it can be increased for low values of P_a/P_f by: (a) using a more sensitive wattmeter element for measuring the reflected power (readily available); (b) reducing the power and increasing the coupling between the specimen and the field generator to increase P_r/P_f ; or (c) choosing the initial operating point higher on the characteristic curve.

5.2 Increasing the Sensitivity. The latter method of increasing the measurement sensitivity involves adjusting the input impedance of the field generator, Z_L , to an initial value greater than 50 ohms prior to placing the biological specimen in the generator. The resulting relationship between P_r/P_f and P_a/P_f can be determined by rewriting eq. (11) as

$$\frac{P_a}{P_L} = 1 - \frac{Z'_L}{N} , \quad (19)$$

where $N = Z_L/50$. Z'_L is limited to real values in the range $0 \leq Z'_L \leq N$. Equation (12) is then substituted into eq. (19) and

the result multiplied by eq. (8), giving

$$\frac{P_a}{P_f} = \frac{(N-1) - 2\Gamma - (N+1)\Gamma^2}{N}, \quad (20)$$

where Γ is limited to real values in the range $-1 \leq \Gamma \leq \frac{N-1}{N+1}$.

Using eq. (6), eq. (20) can be written

$$\frac{P_a}{P_f} = \frac{(N-1) \pm 2\sqrt{P_r/P_f} - (N+1)(P_r/P_f)}{N}, \quad (21)$$

where the (+) sign is used when Γ is negative ($Z_L < 50 \Omega$), and the (-) sign when Γ is positive ($Z_L > 50 \Omega$).

The rf power meters used in this technique, of course, cannot distinguish between positive and negative values of Γ , so that some other means must be employed. One such simple technique would be to slowly increase the value of Z_L . If this causes P_r to increase, then $Z_L > 50 \Omega$. If an increase in Z_L causes a decrease in P_r , then $Z_L < 50 \Omega$.

Equation (21) is shown plotted in figure 5 for values of $N = 1, 2, 3, 5, 10$, and ∞ , for the permissible range of values of Γ given for eq. (20). The upper part of each curve results from negative values of Γ , and the lower part from positive values. As can be seen, the measurement sensitivity (when $P_a/P_f = 0$) has a value of $\delta = 0$ when $N = 1$, increasing to a limiting value of $\delta = 1$ as N is increased. This represents an improvement in sensitivity for values of $P_a/P_f < 0.5$.

As can be seen from figure 5, the reflected power (caused by the initial mismatch) is given by the intercept of each curve with the $P_a/P_f = 0$ axis. These values of P_r/P_f can be determined from the expression,

$$\frac{P_r}{P_f} = \left[\frac{N-1}{N+1} \right]^2, \quad (22)$$

and are 0.000, 0.111, 0.250, 0.444, 0.669, and 1.000, respectively, for the values of $N = 1, 2, 3, 5, 10$, and ∞ . The measurement

sensitivity can be determined approximately from the inverse slope of each curve at its intercept point. As the biological specimen is introduced into the field generator, Z_L will decrease in value, improving the match. This technique should probably be investigated further and may require modification of the present tuning procedure used with the near-field synthesizer.

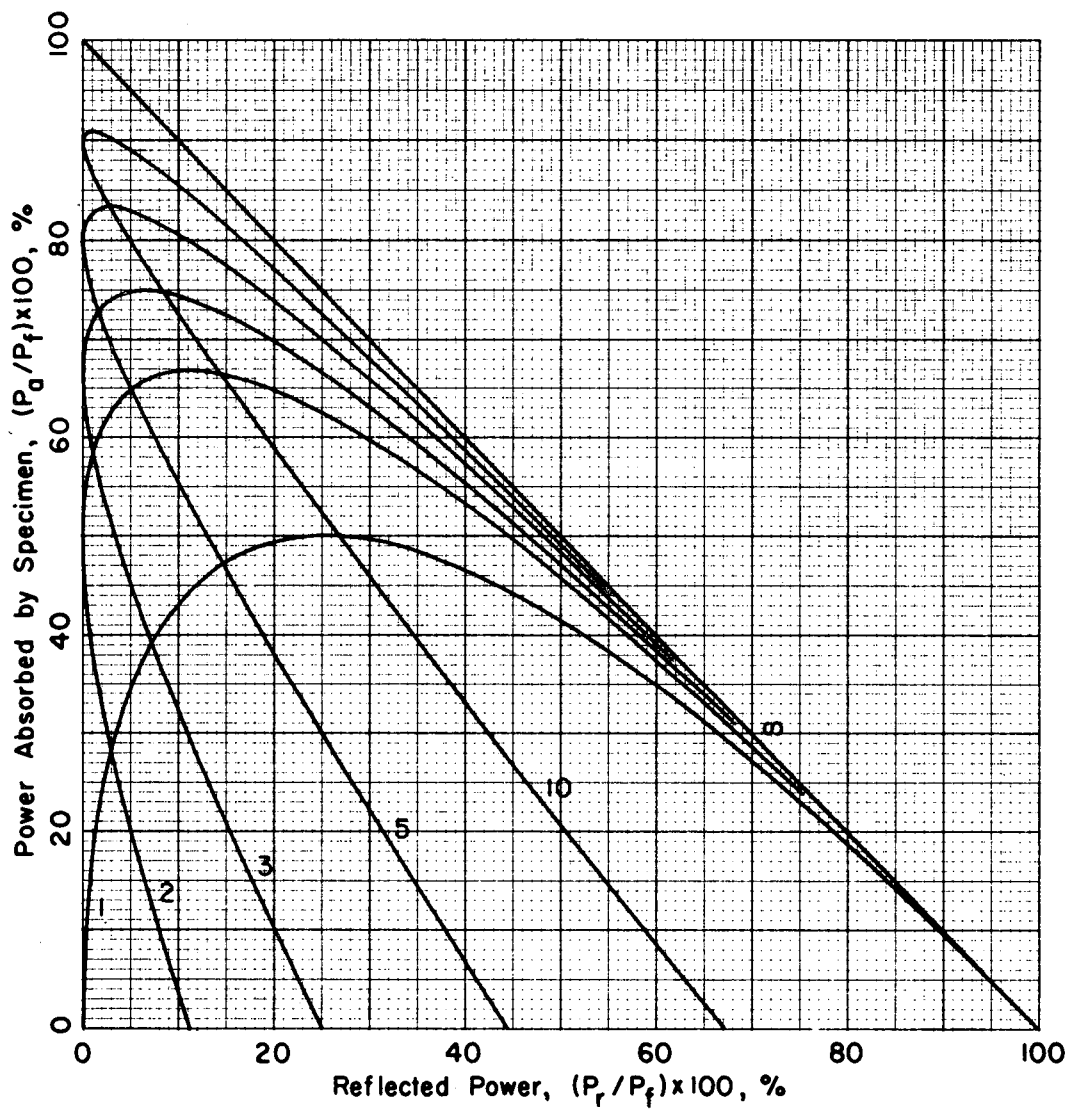


Figure 5. RF power absorbed by the biological specimen, $(P_a/P_f) \times 100, \%$, vs. the reflected power, $(P_r/P_f) \times 100, \%$, for values of $N = 1, 2, 3, 5, 10$, and ∞ , where $N = Z_L/50$ from eq. (19).

6. MAGNETIC-INDUCTION HEATING IN A LOSSY DIELECTRIC

6.1 Introduction. The quasi-static "magnetic-induction" heating caused by an essentially uniform rf magnetic field, H , in a homogeneous, lossy dielectric of permittivity, ϵ , and conductivity, σ , will be determined in this section. The dielectric specimen is in the form of a right circular cylinder of radius, r , and height, h , as shown in figure 6, with H parallel to the axis of the cylinder. The dimensions involved in the dielectric are assumed to be small compared with the operating wavelength. As pointed out previously, the heating caused by the magnetic component of the field may often be greater than that caused by the electric component in the frequency range under consideration here [2].

6.2 Theoretical Background. The electric field, E , and the magnetic field, H , within the dielectric are related at any point by Maxwell's equation

$$\nabla \times E = - \frac{\partial B}{\partial t} . \quad (23)$$

Integrating eq. (23) over the cross-sectional area of the cylinder, $A = \pi r^2$, and applying Stokes's theorem gives, if H is varying sinusoidally in time,

$$\oint_0^{2\pi r} E \cdot d\ell = -j\omega\mu H A, \quad (24)$$

or

$$2\pi r E_\phi = -j\omega\mu H_z A. \quad (25)$$

It should be noted that eq. (24) and eq. (25) are independent of the dielectric properties of the cylinder.

Solving eq. (25) for the magnitude of the electric field gives

$$|E| = \frac{\omega\mu H r}{2} . \quad (26)$$

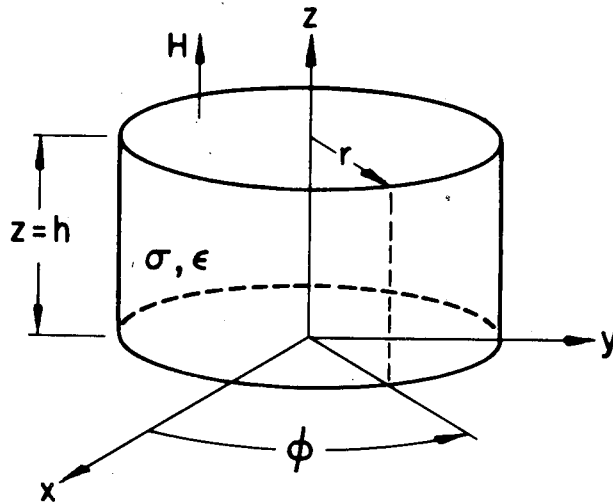


Figure 6. The geometry of the lossy dielectric specimen is in the form of a right circular cylinder of radius, r , and height, h , with H parallel to the axis of the cylinder.

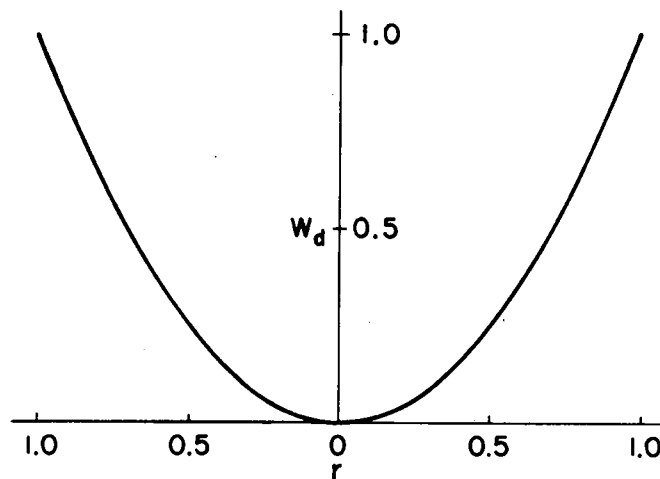


Figure 7. Normalized radial variation of the density of the rf heating, W_d , in a cylindrical lossy dielectric specimen from eq. (28), with H parallel to the axis of the cylinder.

The electric-field lines are in the form of closed circles concentric with the axis of the cylinder and lie in planes normal to H. As can be seen, the magnitude of E is proportional to the radius of the circular E-line in question.

6.3 RF-Heating Density. The density of the rf heating in the dielectric cylinder is given by

$$W_d = E^2 \sigma, \quad W/m^3. \quad (27)$$

The component of the rf heating due to the magnetic field within the cylinder can be determined by substituting eq. (26) in eq. (27), giving

$$W_d = \frac{\sigma \omega^2 \mu^2 H^2 r^2}{4}, \quad W/m^3. \quad (28)$$

Note that the resulting density of the rf heating, and hence the hazard, is proportional to ω^2 , and H^2 , and is independent of the dielectric constant, ϵ , of the specimen. As can be seen, this heating is not uniformly distributed within the cylindrical specimen, but is zero along the axis and increases as the square of the radius, r , as indicated by eq. (28) and shown in figure 7. There is no variation in W_d in either the ϕ or z directions.

Equation (28) neglects internal thermal-conduction processes within the specimen, including blood flow in the case of living tissue, which tend to equalize differences in the heat distribution. Thermal radiation must also be taken into account as indicated later in eq. (33) of section 7. In a practical sense, the total rf heating within the specimen may be more meaningful than the rf heating density, since the former averages the rf heating density and may correlate better with the actual temperature rise within the specimen.

6.4 Total RF Heating. The total rf heating in the dielectric cylinder will now be determined. The heating, dW , in a differential volume, dV , is given by

$$dW = E^2 \sigma dV = E^2 \sigma r dr d\phi dz. \quad (29)$$

Substituting eq. (26) in eq. (29) gives

$$dW = \frac{\sigma \omega^2 \mu^2 H^2 r^3}{4} dr d\phi dz. \quad (30)$$

Integrating eq. (30) over the volume of the dielectric cylinder, gives for the total rf heating,

$$W_t = \frac{\sigma \omega^2 \mu^2 H^2 \pi r^4 h}{8}, \text{ watts.} \quad (31)$$

Note that the total heating is proportional to r^4 , whereas the heating density given by eq. (28) is proportional to r^2 .

Example

Assume the following values for the various parameters in eq. (31):

$$\sigma = 1 \text{ mho/m (1\% saline solution);}$$

$$\epsilon_r = 80;$$

$$f = 26 \times 10^6, \text{ Hz;}$$

$$\mu = 4\pi \times 10^{-7}, \text{ H/m;}$$

$$H = 50 \text{ A/m (rms);}$$

$$r = 0.1 \text{ m; and}$$

$$h = 0.1 \text{ m.}$$

The total heating, W_t , generated in the dielectric cylinder due to the value of magnetic field assumed above is 414 watts. It is interesting to note that over 90 percent of this total heat is developed in the outer half of the cylinder radius, as determined from eq. (31), or that half of the heat is developed in the outer 16 percent of the radius.

7. THE CALORIMETER METHOD

The value of the rf power absorbed by a specimen can be verified using a calorimeter technique if a one-percent saline (Ringer's) solution [10] is used as the specimen. This test solution (made up with distilled water) should be used at room temperature in a low-dielectric-constant polyfoam-insulated container. The walls should have a thickness of 2.5 cm or more to minimize heat loss due to thermal convection. The rf power being absorbed by the solution (in the absence of thermal radiation and convection) is given by

$$W = 69.77 w(T_2 - T_1) / (t_2 - t_1), \quad (32)$$

where W = net power absorbed by the water, watts.

w = weight of the water, kg.

$(T_2 - T_1)$ = temperature increase of the water, °C.

$(t_2 - t_1)$ = elapsed time of the experiment, minutes.

If the weight of the water is 3.14 kg, from the example in section 6; $W = 414$ watts; and $t_2 - t_1 = 1$ min; the resulting temperature rise will be 1.89°C. Due to the small temperature rise involved, the effect of thermal radiation can be shown to be negligible from the Stefan-Boltzmann equation for black-body radiation [11]

$$W_{bb} = \sigma T^4, \quad W/m^2, \quad (33)$$

where $\sigma = 5.672 \times 10^{-8}$, and T = absolute temperature, K.

This will provide a worst-case test since a black-body radiates more than any other at or near room temperature. The body is in thermal equilibrium when its surroundings are at room temperature, T_1 . The net radiation will therefore be proportional to the difference of the fourth powers of the two absolute temperatures involved, T_1 and T_2 , where $T_2 = T_1 + 1.89^\circ$, from the above example. This gives a value of $W_{bb} = 1.11$ watts (for a surface area of 0.126 m^2) which is negligible compared to the 414 watts used in the above example.

8. CONCLUSIONS

A relatively simple method is described in this report for accurately determining the rf power being absorbed by a biological specimen during radiation exposure testing in the frequency range 10 to 100 MHz. The method will permit researchers to monitor rf power flow into the specimen measuring solely forward and reflected power on the feed line to the field generator with conventional rf wattmeters. The measurement accuracy is limited only by the quality of the directional couplers used. A commercially available automatic data-acquisition system can be used to "read" the meters and rapidly calculate, display, and record the rf power flow.

The method has the advantage that the exact measuring point on the feed line is not critical, as it is with methods employing direct impedance measurements. The required forward-and reflected-power measurements can be made at a full operating rf power level of several hundred watts without interfering with the exposure tests. Additional measurements to determine the effect of changes in the field distribution within the field generator, caused by the presence of the biological specimen, would be helpful.

9. REFERENCES

- [1] Greene, F.M., Development and Construction of an Electromagnetic Near-Field Synthesizer, NBS Technical Note 652 (May 1974). For sale by the Superintendent of Documents, U.S. Government Printing Office, Washington, D.C. 20402 (Order by SD Catalog No. C13.46:652) \$0.50.
- [2] Guy, A.W., Electromagnetic Power Deposition in Man Exposed to High-Frequency Fields and the Associated Thermal and Physiologic Consequences (University of Washington, Seattle, Washington 98105). Report SAM-TR-73-13 to USAF School of Aerospace Medicine, Brooks Air Force Base, Texas 78235 (December 1973).
- [3] Terman; F.E., Electronic and Radio Engineering, pp. 466-473 (McGraw-Hill Book Co., Inc., New York, N.Y., 1955).
- [4] Guillemin, E.A., Communication Networks, Vol. II, pp. 33-79 (John Wiley & Sons, Inc., New York, N.Y., 1935).
- [5] Ramo, S., Whinnery, J.R., and VanDuzer, T., Fields and Waves in Communication Electronics, pp. 23-53 (John Wiley & Sons, Inc., New York, N.Y., 1965).
- [6] Ibid., pp. 565-568.
- [7] Montgomery, C.G., Dicke, R.H., and Purcell, E.M., Principles of Microwave Circuits, M.I.T. Radiation Laboratory Series, Vol. 8, p. 367 (McGraw-Hill Book Co., Inc., New York, N.Y., 1948).
- [8] Terman, F.E., op. cit., pp. 44-57.
- [9] IEEE Standard Dictionary of Electrical and Electronics Terms, p. 520. The Institute of Electrical and Electronics Engineers, Inc. (John Wiley & Sons, Inc., New York, N.Y., 1972).
- [10] Kall, A.R., Radiation Hazards Caused by High-Power, High-Frequency Fields, p. III-27 (Ark Electronics Corporation, Willow Grove, Pennsylvania) report to United States Information Agency, Washington, D.C. (June 1968).
- [11] Machol, R.E., System Engineering Handbook, p. 16-3 (McGraw-Hill Book Co., Inc., New York, N.Y., 1965).



HEALTH, EDUCATION, AND WELFARE

PUBLIC HEALTH SERVICE

CENTER FOR DISEASE CONTROL

NATIONAL INSTITUTE FOR OCCUPATIONAL SAFETY AND HEALTH

ROBERT A. TAFT LABORATORIES

4676 COLUMBIA PARKWAY, CINCINNATI, OHIO 45226

OFFICIAL BUSINESS

PENALTY FOR PRIVATE USE. \$300



POSTAGE AND FEES PAID
U.S. DEPARTMENT OF H.E.W.
HEW 399